Stellar populations of early-type galaxies in the ATLAS^{3D} sample

P. Serra[*], R. M. McDermid[†], K. Alatalo[**], L. Blitz[**], M. Bois[‡],
F. Bournaud[§], M. Bureau[¶], M. Cappellari[¶], R. L. Davies[¶], T. A. Davis[¶],
P. T. de Zeeuw[‖,††], E. Emsellem[‡], J. Falcón-Barroso[‡‡], S. Khochfar[§§],
D. Krajnović[¶], H. Kuntschner[¶¶], P.-Y. Lablanche[‡], R. Morganti[*],
T. Naab[***], M. Sarzi[†††], N. Scott[¶], R. C. E. van den Bosch[‡‡‡],
G. van de Ven[§§§], A. Weijmans[††] and L. M. Young[¶¶¶]

[*]*Netherlands Foundation for Research in Astronomy (ASTRON), Postbus 2, 7990 AA Dwingeloo, The Netherlands*
[†]*Gemini Observatory, Northern Operations Centre, 670 N. A'ohoku Place, Hilo, Hawaii 96720, USA*
[**]*Department of Astronomy and Radio Astronomy Laboratory, University of California, Berkeley, CA 94720, USA*
[‡]*Université de Lyon, France; Université Lyon 1, F-69007; CRAL, Observatoire de Lyon, F-69230 Saint Genis Laval; CNRS, UMR 5574; ENS de Lyon, France*
[§]*Laboratoire AIM, CEA-Saclay/DSM/IRFU/SAp - CNRS - Université Paris Diderot, 91191 Gif-sur-Yvette, France*
[¶]*Denys Wilkinson Building, University of Oxford, Keble Road, Oxford OX1 3RH, UK*
[‖]*European Southern Observatory, Karl-Schwarzschild-Str 2, 85748 Garching, Germany*
[††]*Sterrewacht Leiden, Leiden University, Postbus 9513, 2300 RA Leiden, the Netherlands*
[‡‡]*European Space and Technology Centre (ESTEC), Keplerlaan 1, Postbus 299, 2200 AG Noordwijk, the Netherlands*
[§§]*Max-Planck-Institute for Extraterrestrial Physics, Giessenbachstrae ,85748 Garching Germany*
[¶¶]*Space Telescope European Coordinating Facility, European Southern Observatory, Karl-Schwarzschild-Str 2, 85748 Garching, Germany*
[***]*Universitäts-Sternwarte München, Scheinerstr. 1, D-81679 München, Germany*
[†††]*Centre for Astrophysics Research, University of Hertfordshire, Hatfield, Herts AL1 09AB, UK*
[‡‡‡]*McDonald Observatory, The University of Texas at Austin, TX 78712, Austin, USA*
[§§§]*Institute for Advanced Study, Peyton Hall, Princeton, NJ 08544, USA*
[¶¶¶]*Department of Physics, New Mexico Institute of Mining and Technology, Socorro, NM 87801, USA*

Abstract. ATLAS^{3D} is a multi-wavelength, volume-limited survey of 263 morphologically-selected early-type galaxies within a distance of 42 Mpc and complete to $M_K \leq -21.5$. Here we present the ATLAS^{3D} project and our first results on the stellar populations of galaxies in the ATLAS^{3D} sample based on SAURON integral-field spectroscopy. We show relations between integrated line-strength indices and stellar velocity dispersion σ in the range $55 \leq \sigma(\text{km/s}) \leq 350$. We derive simple-stellar-population-equivalent age, metallicity and α/Fe abundance ratio and discuss their relation to stellar velocity dispersion, environment and galaxy internal kinematics. These preliminary results indicate that slow rotators tend to be older and have less variation in age than fast rotators. We also find that galaxies in lower density environments are on average younger than those in denser environments, as found by other authors.

Keywords: Early-type galaxies
PACS: 98.52.Eh

ATLAS^{3D} AND THE ASSEMBLY OF EARLY-TYPE GALAXIES

Early-type galaxies (ETGs) are stellar systems with no evidence of spiral arms and in many cases dominated by a spheroidal stellar component. They are a fundamental group within the galaxy population since they contain most of the stellar mass of the local Universe [1] and dominate the red sequence on the colour-magnitude diagram [2]. ETGs are seen as the end product of the hierarchical assembly, likely the dominant mode of galaxy evolution.

There exist two main approaches to the fundamental questions of the formation and evolution of ETGs. On the one hand, modern telescopes allow us to observe ETGs up to high redshift and therefore directly probe their evolution over cosmic time [e.g., 3]. On the other hand, only low-redshift galaxies can be observed with high S/N ratio at good spatial resolution and so be analyzed in detail. For this reason, much effort has gone in exploiting nearby-ETG data to extract, from their current properties, a record of their past assembly [e.g., 4]. The latter is the approach taken by the ATLAS^{3D} project.

ATLAS^{3D} (http://www-astro.physics.ox.ac.uk/atlas3d) is a complete, multi-wavelength, volume-limited survey of 263 nearby ETGs, supported by numerical simulations and semi-analytic models of galaxy assembly. The ATLAS^{3D} sample is selected on the basis of optical morphology from a parent sample of 844 galaxies (of all types) meeting the criterions *distance* $\leq$42 Mpc and $M_K \leq -21.5$ (with additional constraints on declination and galactic latitude). The morphological classification is based on the (non-) detection of spiral arms in optical images taken from SDSS DR6 (available for 82% of the parent-sample) or DSS2-blue. A detailed description of the sample selection and its characterisation in terms of, for example, luminosity function, distribution on the colour-magnitude diagram and environment can be found in Cappellari et al. (in prep.). Nearly all ATLAS^{3D} galaxies lie on the bright part of the red sequence defined in [1]. The Virgo cluster of galaxies is included in the sample, so that we span a factor of $\sim 10^3$ in environment density. The luminosity function of the sample follows that of larger, z$\sim$0 samples [e.g., 5].

Data taken within ATLAS^{3D} include optical integral-field spectroscopy with SAURON; molecular-gas, millimetre, single-dish observations with IRAM and interferometric follow-up of detections with CARMA; and neutral-hydrogen 21-cm interferometry with the WSRT. Furthermore, INT SDSS-like imaging has been obtained for ATLAS^{3D} galaxies outside the SDSS coverage.

This large data-set allows us to study in a complete fashion stellar content, multi-phase gas content and dynamics of ETGs, and to compare the observations to predictions of numerical simulations and semi-analytic models developed within the team. We will test on solid statistical grounds the results obtained within the SAURON project [e.g., 6], where it was showed that ETGs can be divided in two main families (slow and fast rotators) on the basis of their specific angular momentum, and that these are characterised by different structure as well as stellar and gas content.
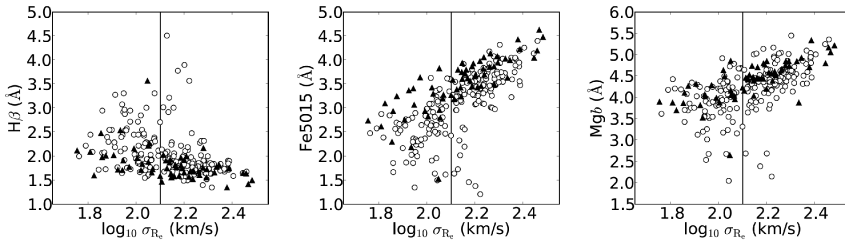
FIGURE 1. Line-strength indices plotted against stellar velocity dispersion for all galaxies in the ATLAS^{3D} sample. Filled triangles and open circles correspond to Virgo and non-Virgo galaxies respectively. The black vertical line is drawn at σ=125 km/s.

STELLAR POPULATIONS IN ATLAS^{3D}

Stellar populations offer an ideal tool to carry out galaxy archeology since they preserve, locked in their age and chemical composition distribution, a memory of the formation of galaxy stellar matter. Our SAURON integral-field spectroscopy provides a panoramic view of the distribution of stellar populations across galaxies within the inner effective radius (R_e). In this proceeding, we show preliminary results on the stellar populations in ATLAS^{3D} galaxies from integrated spectra within a circular aperture of one R_e.

We study stellar populations by measuring from the spectra line-strength indices on the Lick/IDS system after having removed the ionised-gas emission lines as explained in [7]. We then compare the observed line-stregth indices Hβ, Fe5015 and Mgb to predictions of simple-stellar-population (SSP) models by [8]. This allows us to derive SSP-equivalent age, metallicity and [α/Fe] abundance ratio for all galaxies.

In figure 1 we show line-strength indices plotted against the stellar velocity dispersion measured from our spectra. In the figure, filled triangles and open circles correspond to Virgo and non-Virgo galaxies respectively. The vertical line shows the lowest velocity dispersion probed by [4], the largest compilation of long-slit literature data of nearby ETGs analysed to date. ATLAS^{3D} pushes the study of stellar populations in ETGs down to much lower galaxy mass over large, self-consistent apertures for a complete, volume-limited sample (and employing integral-field rather than long-slit spectroscopy). This is a fundamental improvement over previous work that allows, among other studies, a more thorough comparison to the scaling relations predicted by models of galaxy formation (e.g., [α/Fe] vs. σ in [9]).

Figure 1 extends to lower σ the general trend according to which small ETGs have on average larger Hβ and lower metal-index values (and are on average younger, more metal-poor and less [α/Fe]-enhanced) than massive galaxies [e.g., 4]. However, the scatter in the index-σ relations (and in the derived stellar parameter-σ relations) increases significantly at $\sigma \leq 100$ km/s, possibly indicating a larger diversity of star-formation

113

histories. Intermediate SSP-equivalent ages ranging from 0.5 to 3 Gyr and low $[\alpha/\text{Fe}]$ values are much more frequent, over our 1-R_e apertures, at $\sigma \leq 100$ km/s than at larger σ values. This indicates recent formation of a detectable fraction of the stellar mass of small ETGs even when examining galaxy spectra over such extended regions. Smaller aperture and composite-stellar-population analysis are natural extensions of this preliminary study.

We analyse also the relation between stellar populations and environment. Figure 1 shows how non-Virgo galaxies (open circles) have on average larger Hβ and slightly lower Fe5015 and Mgb values than Virgo galaxies (filled triangles). The derived SSP-equivalent stellar-population parameters confirm that galaxies in the Virgo cluster are on average older than non-Virgo galaxies (i.e., ETGs in field and small groups) while showing roughly comparable [Z/H] and $[\alpha/\text{Fe}]$.

We make use of a preliminary classification of ETGs in the ATLAS^{3D} sample in slow and fast rotators [see 6] to study the stellar populations in these two classes. Slow rotators are typically massive, old galaxies (although we find a few at low σ). Fast rotators cover evenly the whole σ range and extend towards younger SSP-equivalent ages and lower $[\alpha/\text{Fe}]$. It is interesting to find some slow rotators (usually ETGs that experienced numerous merging, including dissipationless merging, through their assembly history) at the lowest [Z/H] and environmental density. Further work is necessary to understand the role of these objects over the observed ETG mass range.

Along with the sample size and selection, which makes it possible to compare our results to the predictions made by models of galaxy formation, the other major improvement allowed by ATLAS^{3D} over previous work is the extension of the integral-field spectroscopic technique (proved successful by the SAURON project) to a large, complete sample. This will enable us to correlate stellar population features to morphology, kinematics and ISM properties, including neutral (both molecular and atomic) and ionised gas. Such a combination of data is fundamental to understand the origin of the variety of features found in ETGs and interpret them as clues on their formation process.

REFERENCES

1. I. K. Baldry, et al., *ApJ* **600**, 681–694 (2004), `arXiv:astro-ph/0309710`.
2. A. J. Benson, D. Džanović, C. S. Frenk, and R. Sharples, *MNRAS* **379**, 841–866 (2007).
3. E. F. Bell, et al., *ApJ* **608**, 752–767 (2004), `arXiv:astro-ph/0303394`.
4. D. Thomas, C. Maraston, R. Bender, and C. Mendes de Oliveira, *ApJ* **621**, 673–694 (2005), `arXiv:astro-ph/0410209`.
5. E. F. Bell, D. H. McIntosh, N. Katz, and M. D. Weinberg, *ApJS* **149**, 289–312 (2003), `arXiv:astro-ph/0302543`.
6. E. Emsellem, et al., *MNRAS* **379**, 401–417 (2007), `arXiv:astro-ph/0703531`.
7. M. Sarzi, et al., *MNRAS* **366**, 1151–1200 (2006), `arXiv:astro-ph/0511307`.
8. D. Thomas, C. Maraston, and R. Bender, *MNRAS* **339**, 897–911 (2003), `arXiv:astro-ph/0209250`.
9. A. Pipino, and F. Matteucci, *MNRAS* **347**, 968–984 (2004), `arXiv:astro-ph/0310251`.